Available Online at http://www.journalajst.com

ASIAN JOURNAL OF SCIENCE AND TECHNOLOGY

ISSN: 0976-3376

Asian Journal of Science and Technology
Vol. 14, Issue, 10, pp. 12745-12750, October, 2023

RESEARCH ARTICLE

NUMERICAL ANALYSIS OF NATURAL CONVECTION AND INFLUENCE OF THE COLLECTOR RADIUS ON THE VELOCITY AND TEMPERATURE FIELDS IN A SOLAR TOWER WITHOUT TURBINE

Moctar Ousmane*[1], Boureima Kaboré[2], Germain Wende Pouiré Ouedraogo[3], Salifou Ouédraogo[4], B. Magloire Pakouzou[5], Thierry Sikoudouin Maurice KY[4], Dianda Boureima[4,6], KAM Sié[4] and Dieudonné Joseph Bathiébo[4]

[1,4]University of Agadez, PO BOX 199, Niger; [2]Département de Physique, UFR-ST, Université Norbert ZONGO/Koudougou; [3]Université de Fada N'Gourma; [4]Laboratory L.E.T.R.E, University Joseph KI-ZERBO, Ouagadougou 03 PO BOX, 7021, Burkina Faso; [5]Université de Bangui (Centrafrique); [6]Institute of Research in Applied Science and Technologies, Ouagadougou 03 PO Box 7047, Burkina Faso

ARTICLE INFO

Article History:
Received 11th July, 2023
Received in revised form
21st August, 2023
Accepted 06th September, 2023
Published online 27th October, 2023

Keywords:
Solar tower, Natural convection, Collector radius, Comsol.

ABSTRACT

In this paper, we present a numerical analysis of natural convection and the effects of collector radius variation on the velocity and temperature field. After transforming the conservation equations of mass, momentum and energy, we compare the results of our calculation code with those of Comsol. On the one hand, the comparative study of the temperatures in the collector reveals a slight difference at the entrance to the chimney, on the other hand we note that there is a perfect agreement with the general appearance of the evolution curves temperatures in the chimney. In addition, the evolution of speeds in the collector suggests the choice of a tighter mesh. We also note very low velocity values in the chimney. In addition we also present some velocity and temperature profiles in the flow as a function of the Rayleigh number. Finally, a variation in pressure during the flow was studied.

Citation: ***Moctar Ousmane, Boureima Kaboré, Germain Wende Pouiré Ouedraogo, Salifou Ouédraogo, B. Magloire Pakouzou, Thierry Sikoudouin Maurice KY, Dianda Boureima, KAM Sié and Dieudonné Joseph Bathiébo.*** **2023.** "Numerical analysis of natural convection and influence of the collector radius on the velocity and temperature fields in a solar tower without turbine", *Asian Journal of Science and Technology*, 14, (10), 12745-12750.

INTRODUCTION

The solar chimney is a new technology for producing electricity by transforming solar energy into mechanical energy. The basic idea comes from Jörg Schlaich and Rudolf Bergermann in 1976 [1]. They developed a prototype which operated from 1982 to 1989. Since then, the reliability of the system has aroused the enthusiasm of researchers, industrialists and political decision-makers. It is made up of three main parts: the collector (either plastic or glass or both combined), the chimney and the turbine. The principle diagram is given by Figure 1. Bernades et al. [2] used computational fluid simulation (CFD) to simulate the flow in a solar chimney under natural convection in a radial flow. They studied the different junction shapes at the base of the collector to predict the thermo-hydrodynamic behavior. Sangi et al [3] also concluded that the power output increases directly if the height of the stack and the diameter of the collector also increases. Ayadi. A. et al. [4,5] conducted an experimental study on the effect of chimney height and collector roof inclination on the performance of a solar tower. Yilmaz et al. [6] concluded that the most important factor affecting the performance of solar chimneys was tower height and collector area. Al-Azawiey et al. [7] experimentally studied a solar tower prototype with a chimney of 6.3 m height and 0.32 m diameter, collector diameters of 3 m and 6 m. They showed that the air velocity in the chimney was 1.56 m/s for a collector diameter of 3 m, and 2.25 m/s for a collector diameter of 6 m under sunlight of 808 W/m^2. They further noted that by doubling the diameter of the chimney the air flow in the chimney increases byapproximately 44.23%. Zhou et al. [8] then [9,10,11,12,13] developed a mathematical model and showed that an increase in the collector radius leads to an increase in the output power. Toghraie et al. [14] after analyzing the effect of geometric parameters on the performance of solar chimneys using 3D CFD model concluded that increasing the collector radius would increase the temperature in the collector. Li et al [15], Choi et al [16] developed a theoretical model which allowed them to find a limiting value of the collector radius beyond which an improvement in the output power is not possible. Rajput et al. [17] undertook a CFD study referring to the Manzanares prototype. They claimed that improving the collector radius improved the turbine inlet air velocity, mass flow rate, and power output. Zhu et al. [18] studied the effect of changing the chimney height of a small-scale prototype with a chimney of 0.7 m diameter and a collector of radius 5 m under a constant radiation of 850 W/m^2 using a mathematical model based on experimental results. They obtained powers of 2.26 W and 4.94 W respectively for chimney heights of 4 m and 8 m. Papageorgiou et al [19] obtained a speed of 5 m/s for a chimney height of 15 m compared to a speed of 6 m/s for a chimney height of 24 m. Bernades et al [20] developed a numerical model which allowed them to assert that by increasing the height of the chimney by 100% they would obtain a daily power output of 2016 GWh compared to 0.929 GWh with 1000 m of chimney height. As for Nizetic et al [21], they developed a numerical model capable of improving the efficiency of the chimney. Thus they obtained 0.698% for a chimney height of 200 m compared to 3.411% for a height of

1000 m. Larbi et al [22] showed the increase in output power for several values of stack heights and collector diameters. Li et al. [23] claimed that the output power of the Manzanares prototype was 53.5 kW under a constant irradiation of 1000 W/m^2, and if the height of the chimney was fixed at 400 m, the output power would be 123.6 kW, an increase of 131%. Hamdan et al [24] showed that a 400 m chimney would produce 5.81 MW under sunlight of 263 W/m2 compared to 16.26 MW for double height. Ngala et al [25] obtained an output power of 1.5.10^9 W for a chimney height of 300 m compared to 3.02.10^9 W for a height of 600 m. Khelifi et al [26] through a numerical model obtained an output power of 1852.57 kW for a chimney height of 200 m compared to 3696.44 kW for 400 m chimney height.

Mathematical formulation: We use the same equations, assumptions and boundary conditions as Ousmane et al. [27] in the temperature range (320 < T < 370) K.

Mass conservation

$$\frac{\partial(V_\xi)}{\partial\xi}+\frac{\partial(V_\eta)}{\partial\eta}=0 \tag{1}$$

Vorticity equation

$$\frac{V_\xi}{h}\frac{\partial w}{\partial\xi}+\frac{V_\eta}{h}\frac{\partial w}{\partial\eta}=\frac{\nu}{h^2}\left(\frac{\partial^2 w}{\partial\xi^2}+\frac{\partial^2 w}{\partial\eta^2}\right)+g\beta\left[A(\xi,\eta)\frac{\partial T}{\partial\xi}+B(\xi,\eta)\frac{\partial T}{\partial\eta}\right] \tag{2}$$

Energy conservation equation

$$V_\xi\frac{\partial T}{\partial\xi}+V_\eta\frac{\partial T}{\partial\eta}=\frac{1}{h}\frac{\lambda}{\rho.Cp}\left(\frac{\partial^2 T}{\partial\xi^2}+\frac{\partial^2 T}{\partial\eta^2}\right) \tag{3}$$

The numerical resolution is identical to that adopted by Ousmane et al. [27] leads to the equations below:

$$\frac{\partial V_\xi^*}{\partial\xi^*}+\frac{\partial V_\eta^*}{\partial\eta^*}=0 \tag{4}$$

$$\frac{\partial}{\partial\xi^*}\left(\frac{1}{H}\frac{\partial T^*}{\partial\xi^*}-V_\xi^* T^*\right)+\frac{\partial}{\partial\eta^*}\left(\frac{1}{H}\frac{\partial T^*}{\partial\eta^*}-V_\eta^* T^*\right)=0 \tag{5}$$

$$\frac{\partial}{\partial\xi^*}\left(\frac{Pr}{H}\frac{\partial w^*}{\partial\xi^*}-V_\xi^* w^*\right)+\frac{\partial}{\partial\eta^*}\left(\frac{Pr}{H}\frac{\partial w^*}{\partial\eta^*}-V_\eta^* w^*\right)=-Pr.Ra\left(C(\xi^*,\eta^*)\frac{\partial T^*}{\partial\xi^*}+D(\xi^*,\eta^*)\frac{\partial T^*}{\partial\eta^*}\right) \tag{6}$$

With

$$w^*=-\frac{1}{H^2}\left(\frac{\partial^2\psi^*}{\partial\xi^{*2}}+\frac{\partial^2\psi^*}{\partial\eta^{*2}}\right) \tag{7}$$

Comparative study of the obtained results with those of the COMSOL code: The calculation code developed makes it possible to estimate temperatures and velocities within the flow. To validate the latter with figures from the "COMSOL" code we present in dimensional variables the variations in temperature and velocities. Note that this choice results from the simple fact that it is easier to compare these curves using real physical quantities.

Evolution of temperatures and Nusselt number in the collector: We evaluate the average systematic errors (RMSE) of our calculation program, for each temperature evolution curve, by comparing it to the results of the COMSOL code.

$$RMSE=\sqrt{\frac{1}{N}\sum_{1}^{N}\left(X_{exp,i}^*-X_{pre,i}^*\right)^2}$$

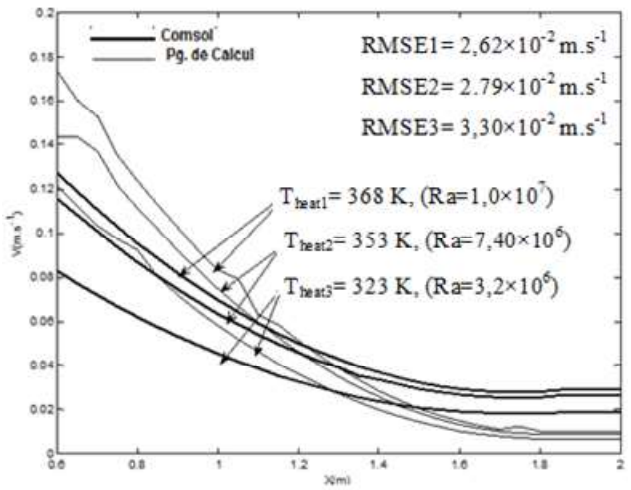

Figure 3. Spatial evolution of velocities in the collector

Temperature evolution in the chimney: Figure 4 shows a perfect agreement between the temperature curves in the chimney with a quasi-hyperbolic profile consistent with literature data [28].

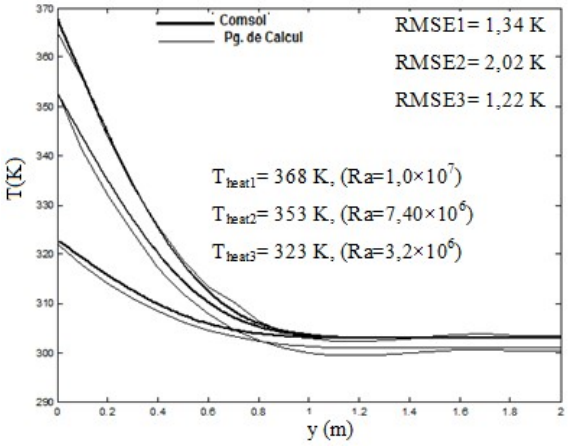

Figure 4. Spatial evolution of temperatures in the chimney

Velocity evolution in the chimney: It can be noted on Figure 5 that this is a very low speed and therefore the errors linked to the discretization of the equations and the use of relaxation coefficients greatly amplify the relative uncertainties in the calculated values. The parabolic profile of the speed curves is in perfect agreement with the literature data confirmed by Nizetic et al [29]. Figure 6 gives an illustration of the characteristics of the flow using graphics from the Comsol calculation code.

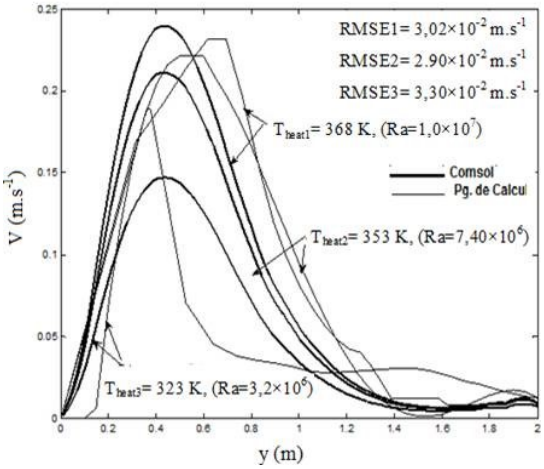

Figure 5. Spatial evolution of velocities in the chimney

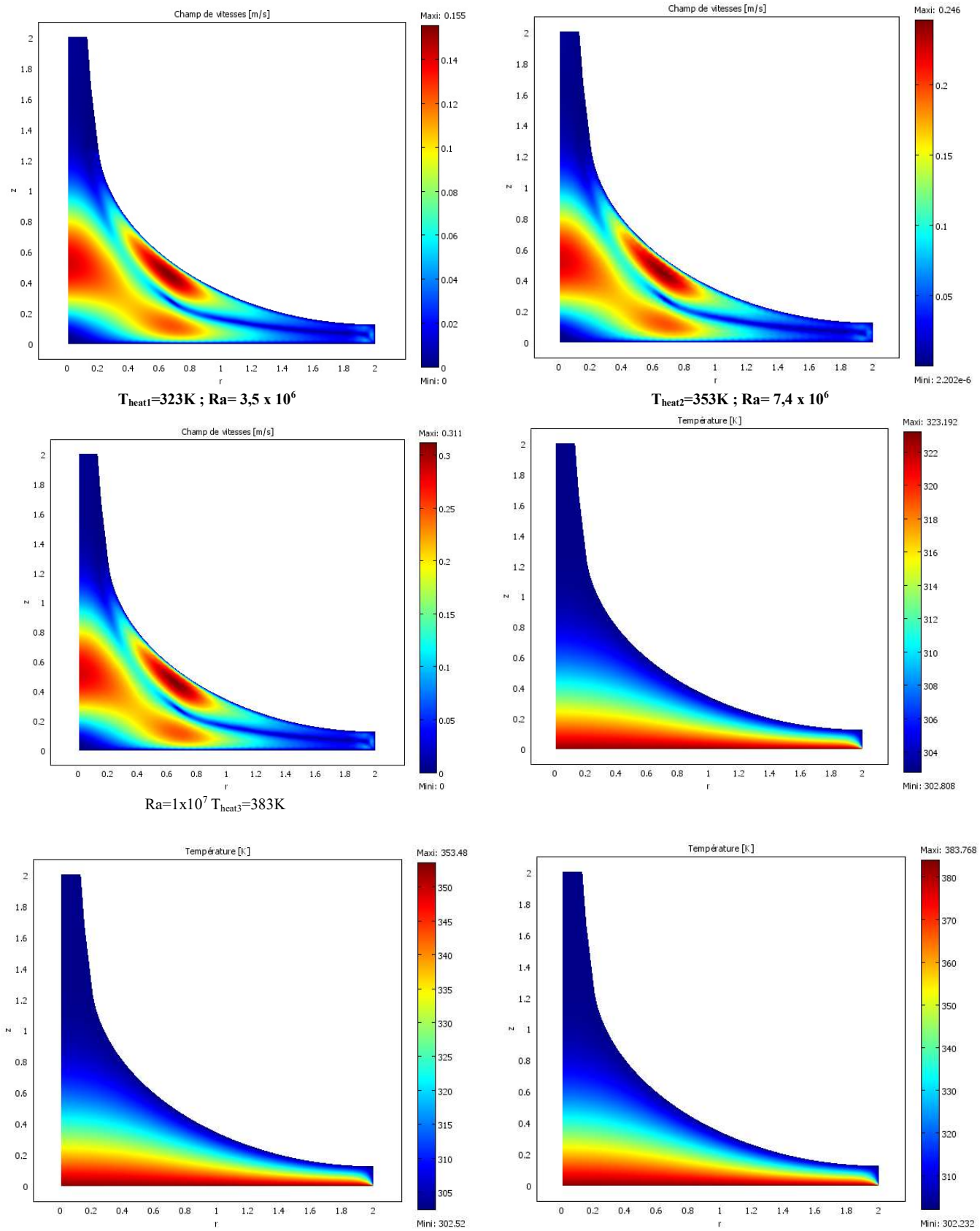

T_{heat1}=323K ; Ra= 3,5 x 10^6

T_{heat2}=353K ; Ra= 7,4 x 10^6

Ra=1x10^7 T_{heat3}=383K

Figure 6. Velocity and temperature profiles in the flow as a function of the Rayleigh number

We notice that "the zone of maximum velocities" keeps practically the same intervals on the ordinate, in particular Hm= (0.2 - 0.6) m or H= (0.1 - 0.3) in dimensionless values whatever the Rayleigh number between 10^6< Ra <10^7. This locus of maximum velocities varies from one geometry to another, thus giving it a compact or spread-out appearance. In fact, the geometry of the tower is more determining as to the position of the "maximum velocity zone".

Visualization of iso temperature values for Theat =353K (Ra=7.4.10^6): Figures 7 to 11 are obtained by simulation for a fixed temperature of the absorber (Theat =353K). The abscissa axis is the radius of the collector because we are moving in axisymmetric and the ordinate axis represents the height of the chimney, i.e. (rc=hch=2m). The convective movements in laminar regime remain quite weak so that we can clearly see the temperature gradient which

is established in the chimney. The separation of the isotherms (bell curves) reflects a laminar convection regime which is established between the two main walls (cold and hot).

Visualization of iso velocities values and streamlines for Theat =353K (Ra=7.4.10^6): The "maximum velocities" zone is well marked and is reflected by concentric circles of iso values whose diameters are between the ordinates (0.25 and 0.65) m. We notice that by traversing the y axis from bottom to top we find the velocity profile in the chimney of Figure 5. At the beginning very low velocities increase suddenly in a Gaussian bell curve to attenuate immediately after and remain practically constant in the rest of the chimney.

Figures 7 and 9 show that the current lines originate at the level of the absorber and part of them undergoes recirculation in contact with the colder wall of the collector. We observe a single convective cell confirming the laminar regime for a Rayleigh number of approximately 10^7. Indeed, multicellular flow (Bénard cells) appears in turbulent regime.

Influence of the collector radius on the velocity and temperature fields: The increase in the radius of the collector is linked to that of the surface of the absorber. The fluid then stays longer in the conduit, therefore heats up much more and makes it possible to obtain higher velocities, as indicated in Figure 10.

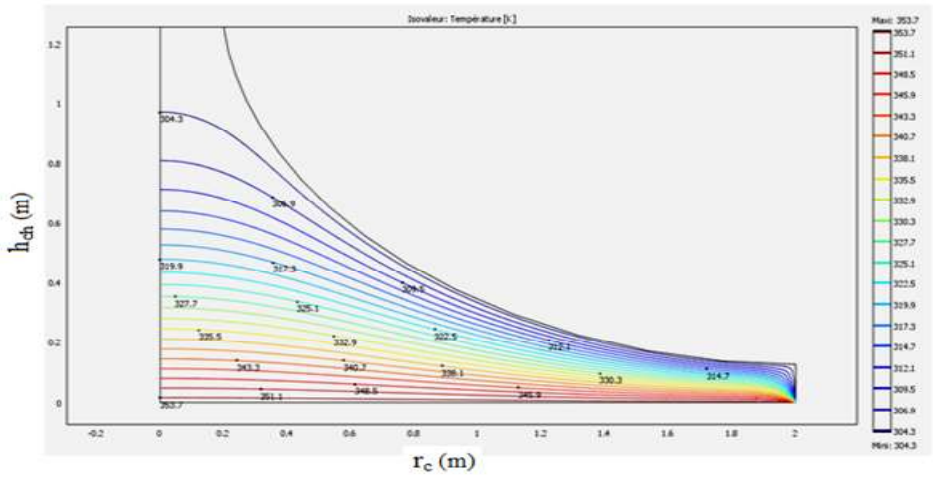

Figure 7. View of iso temperature values for Theat=353K (Ra= 7.4×10^6)

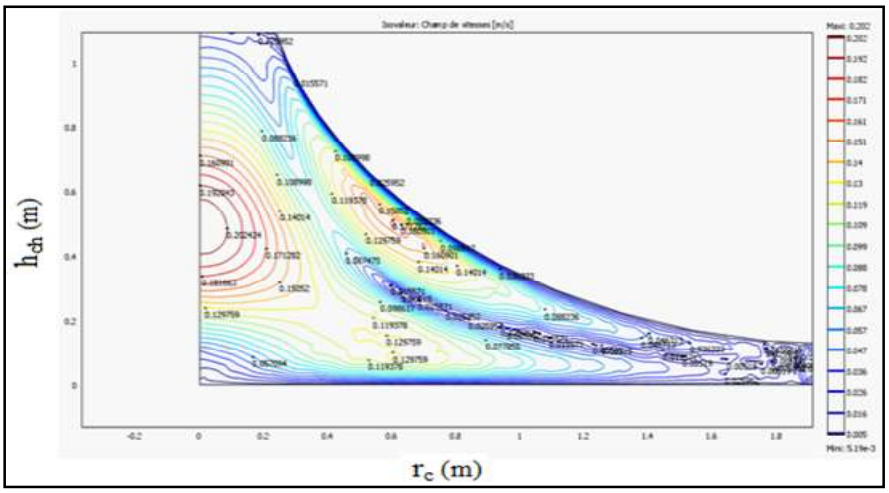

Figure 8. Velocity field

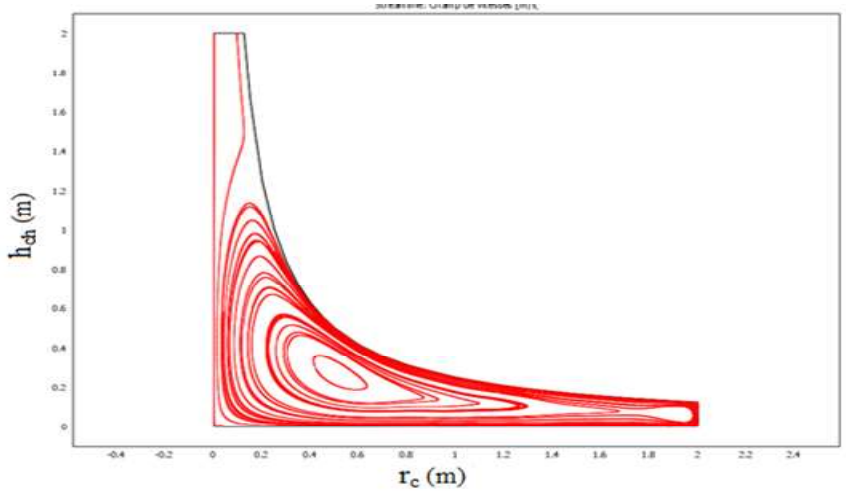

Figure 9. Current lines in laminar regime (Value of the current function)

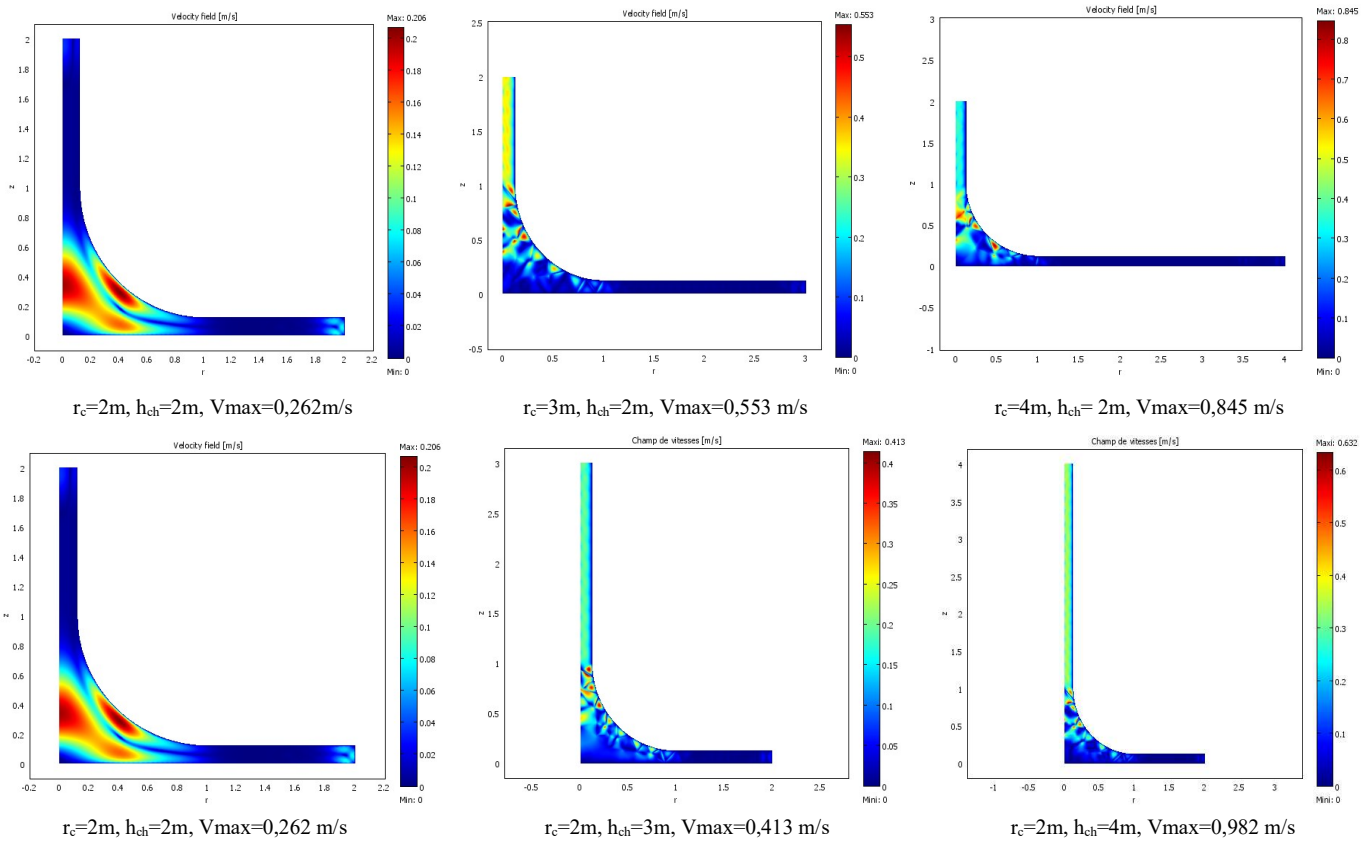

r_c=2m, h_{ch}=2m, Vmax=0,262m/s | r_c=3m, h_{ch}=2m, Vmax=0,553 m/s | r_c=4m, h_{ch}= 2m, Vmax=0,845 m/s

r_c=2m, h_{ch}=2m, Vmax=0,262 m/s | r_c=2m, h_{ch}=3m, Vmax=0,413 m/s | r_c=2m, h_{ch}=4m, Vmax=0,982 m/s

Figure 10. Influence of collector radius and chimney height

Mesh statistics (r_c=2m, h_{ch}=2m)	
Vmax	0,262m/s
Number of degrees of freedom	6303
Number of nodes	174
Number of elements	279
Triangular	279
Quadrilatéral	0
Number of border elements	67
Vertex number	13
Minimum elementquality	0.708
Element area ratio	0.023

Mesh statistics (r_c=3m, h_{ch}=2m)	
Vmax	0,532 m/s
Number of degrees of freedom	1708
Number of nodes	62
Number of elements	68
Triangular	68
Quadrilatéral	0
Number of border elements	54
Vertex number	8
Minimum elementquality	0.798
Element area ratio	0.145

Mesh statistics (r_c=4m, h_{ch}= 2m)	
Vmax	0,845m/s
Number of degrees of freedom	1925
Number of nodes	71
Number of elements	76
Triangular	76
Quadrilatéral	0
Number of border elements	64
Vertex number	7
Minimum elementquality	0.776
Element area ratio	0.113

Mesh statistics (r_c=2m, h_{ch}=2m)	
Vmax	0,262m/s
Number of degrees of freedom	6303
Number of nodes	174
Number of elements	279
Triangular	279
Quadrilatéral	0
Number of border elements	67
Vertex number	13
Minimum elementquality	0.708
Element area ratio	0.023

Mesh statistics (r_c=2m, h_{ch}=3m)	
Vmax	0,661 m/s
Number of degrees of freedom	5993
Number of nodes	183
Number of elements	256
Triangular	256
Quadrilatéral	0
Number of border elements	108
Vertex number	8
Minimum elementquality	0.741
Element area ratio	0.149

Mesh statistics (r_c=2m, h_{ch}=4m)	
Vmax	0,982 m/s
Number of degrees of freedom	1839
Number of nodes	69
Number of elements	72
Triangular	72
Quadrilatéral	0
Number of border elements	64
Vertex number	8
Minimum elementquality	0.588
Ratio de surface de l'élément	0.152

It should be noted that the effect of increasing the radius has a greater impact on the increase in the velocity than the chimney effect because the fluid acquires more thermal energy in the vicinity of the absorber than by natural draft effect.

Pressure variation during flow: Consistent with Sangi et al. [30], the pressure decreases along the collector and its minimum value is located at the bottom of the chimney. Ming et al. [31] showed that this pressure is negative and increases inside the chimney. The observation of Figure 11 proves the good agreement with the literature data.

CONCLUSION

In the collector, we note a perfect agreement between the temperature evolution curves given by COMSOL and our calculation program. However, we observe a slight difference at the entrance to the chimney for the two types of curves. However, the temperature curves in the chimney show perfect agreement between the COMSOL code and the calculation program. The evolution of velocities in the collector presents very small differences at the entrance to the chimney while in the chimney the low velocities result earlier from errors linked to the discretization and the relaxation method. Finally,

the COMSOL code confirms the growth in velocities as a function of the radius of the collector and the height of the chimney, as well as the ascending convective movement described by the pressure curves: the inlet is in depression and the outlet tends towards the jet condition in a free atmosphere.

ACKNOWLEDGEMENT

We are grateful to the International Science Program (ISP) for supporting BUF01.

REFERENCES

Al-Azawiey, S.S.; Al-Kayiem, H.H.; Hassan, S.B. On the Influence of Collector Size on the Solar Chimneys Performance. In Proceedings of the MATECWeb of Conferences, Malacca, Malaysia, 25–27 February 2017; p. 131.

Ayadi, A., Driss, Z., Bouabidi, A., & Abid, M. S. (2017). Experimental and Numerical study of the impact of the collector roof inclination on the performance of a solar chimney power plant. Energy and Building, 139, 263–276. Doi: 10.1016/j.enbuild.2017.01.047

Ayadi, A., Driss, Z., Bouabidi, A., &Nasraoui, H. (2018). A computational and an experimental study on the effect of the chimney height on the thermal characteristics of a solar chimney power plant. Proceedings of the Institution of Mechanical Engineers, Part E: *Journal of Process Mechanical Engineering*, 232(4), 503-516.

Bernardes, M.A.d.S.; Voss, A.; Weinrebe, G. Thermal and technical analyzes of solar chimneys. Sol. Energy 2003, 75, 511–524.

Choi, Y.J.; Kam, D.H.; Park, Y.W.; Jeong, Y.H. Development of analytical model for solar chimney power plant with and without water storage system. *Energy* 2016, 112, 200–207.

Gholamalizadeh, E.; Mansouri, S.H. A comprehensive approach to design and improve a solar chimney power plant: A special case–Kerman project. *Appl. Energy* 2013, 102, 975–982

Guo, P.H.; Li, J.Y.; Wang, Y. Annual performance analysis of the solar chimney power plant in Sinkiang, China. Energy Convers. Manag. 2014, 87, 392–399

Hamdan, M.O. Analysis of solar chimney power plant utilizing chimney discrete model. *Renew. Energy* 2013, 56, 50–54.

Hamdan, M.O. Analysis of solar chimney power plant utilizing chimney discrete model. *Renew. Energy* 2013, 56, 50–5

Khelifi, C.; Ferroudji, F.; Ouali, M. Analytical modeling and optimization of a solar chimney power plant. *Int. J. Eng. Res. Afr.* 2016, 25, 78–88.

Khelifi, C.; Ferroudji, F.; Ouali, M. Analytical modeling and optimization of a solar chimney power plant. *Int. J. Eng. Res. Afr.* 2016, 25, 78–88.

Larbi, S.; Bouhdjar, A.; Chergui, T. Performance analysis of a solar chimney power plant in the southwestern region of Algeria. *Renew. Sustain. Energy Rev.* 2010, 14, 470–477.

Li, J.Y.; Guo, P.H.; Wang, Y. Effects of collector radius and chimney height on power output of a solar chimney power plant with turbines. *Renew. Energy* 2012, 47, 21–28.

Li, J.Y.; Guo, P.H.; Wang, Y. Effects of collector radius and chimney height on power output of a solar chimney power plant with turbines. *Renew. Energy* 2012, 47, 21–28.

M. OUSMANE, B. DIANDA, S. KAM, A. KONFE, T. KY AND D. J. BATHIEBO. Experimental Study in Natural Convection. *Global Journal of Pure and Applied Sciences*. vol. 21, pp. 155 à 169. (2015).

Marco Aurelio dos Santos Bernardes, Ramon Molina Valle, Marcio Fonte-Boa Cortez. Numerical analysis of natural laminar convection in a radial solar heater. *Int. J. Therm. Sci.* (1999) 38, 42-50.

Ming, T., Lui, W., Xu, G., 2006. Analytical and numerical investigation of the solar chimney power plant systems. *Int.J. Energy Res;* 30 : 861-873.8

Moctar Ousmane, Thierry Sikoudouin Maurice Ky, Amadou Konfé, Boureima Dianda, Salifou Ouédraogo,Dieudonné Joseph Bathiébo. Natural Convection Modeling in a Solar Tower. *Indian Journal of Science and Technology,* 2021,14(48)

Ngala, G.M.; Oumarou, M.B.; Muhammad, A.B.; Shuwa, M. Evaluation of solar chimney power plant in semi-arid region of Nigeria. *Arid. Zone J. Eng. Technol. Enviroment*

Ngala, G.M.; Oumarou, M.B.; Muhammad, A.B.; Shuwa, M. Evaluation of solar chimney power plant in semi-arid region of Nigeria. *Arid. Zone J. Eng. Technol. Enviroment* 2015, 11, 1–12.

Nizetic S, Klarin B. A simplified analytical approach for evaluation of the optimal ratio of pressure drop across the turbine in solar chimney power plants. *Appl Energy;* 2010; 87(2), 587–591. DOI: 10.1016/j.apenergy.2009.05.019

Nizetic, S.; Ninic, N.; Klarin, B. Analysis and feasibility of implementing solar chimney power plants in the Mediterranean region. *Energy* 2008, 33, 1680–1690.

Papageorgiou, C.D. Enclosed Solar Chimney Power Plants with Thermal Storage. *Open Access Libr. J.* 2016, 3, 1–18

Rajput, S.R.; Nigam, S.R.; Sen, M. Integrated solar heat, and wind power plant: Design and performance. *Int. J. Eng. Sci. Manag.* 2017, 7, 407–4

Sangi, R. Performance evaluation of solar chimney power plants in Iran. Renew. Sustain. Energy Rev. 2012, 16, 704–710

Sangi, R., Amidpour, M., Hosseinizadeh, B., 2011. Modeling and numerical simulation of Solar chimney power plants. Solar Energy, 85, 829–838.

Toghraie, D.; Karami, A.; Afrand, M.; Karimi-Pour-Fard, A. Effects of geometric parameters on the performance of solar chimney power plants. Energy 2018, 162, 1052–1061.

W. Haaf, K. Friedrich, G. Mayir, J. Schlaich. Solar Chimneys Part I: Principle and construction of the pilot plant in Manzanares. *Int. J. Solar Energy,* (1983) Vol. 2, pp. 3-20

Yilmaz, A., Unvar, S., Avci, A. S., &Aygün, B. (2019). Difference of solar chimney system chimney designs and numerical modeling in collector surface areas. *International Journal of Scientific & Engineering Research*, *10*(9).

Zhou, X.; Wang, F.; Fan, J.; Ochieng, R.M. Performance of solar chimney power plant in Qinghai-Tibet Plateau. *Renew. Sustain. Energy Rev.* 2010, 14, 2249–2255

Zhou, X.; Yang, J.; Xiao, B.; Hou, G. Simulation of a pilot solar chimney thermal power generating equipment. *Renew. Energy* 2007, 32, 1637–1644.

****